Adipose Tissue Endothelial Cells From Obese Human Subjects: Differences Among Depots in Angiogenic, Metabolic, and Inflammatory Gene Expression and Cellular Senescence

Aurélie Villaret,[1,2] Jean Galitzky,[1] Pauline Decaunes,[1] David Estève,[1] Marie-Adeline Marques,[1] Coralie Sengenès,[1] Patrick Chiotasso,[3] Tamara Tchkonia,[4] Max Lafontan,[1] James L. Kirkland,[4] and Anne Bouloumié[1]

OBJECTIVE—Regional differences among adipose depots in capacities for fatty acid storage, susceptibility to hypoxia, and inflammation likely contribute to complications of obesity. We defined the properties of endothelial cells (EC) isolated from subcutaneous adipose tissue (SAT) and visceral adipose tissue (VAT) biopsied in parallel from obese subjects.

RESEARCH DESIGN AND METHODS—The architecture and properties of the fat tissue capillary network were analyzed using immunohistochemistry and flow cytometry. $CD34^+/CD31^+$ EC were isolated by immunoselection/depletion. Expression of chemokines, adhesion molecules, angiogenic factor receptors, as well as lipogenic and senescence-related genes were assayed by real-time PCR. Fat cell size and expression of hypoxia-dependent genes were determined in adipocytes from both fat depots.

RESULTS—Hypoxia-related genes were more highly expressed in VAT than SAT adipocytes. VAT adipocytes were smaller than SAT adipocytes. Vascular density and EC abundance were higher in VAT. VAT-EC exhibited a marked angiogenic and inflammatory state with decreased expression of metabolism-related genes, including endothelial lipase, GPIHBP1, and PPAR gamma. VAT-EC had enhanced expression of the cellular senescence markers, IGFBP3 and γ-H2AX, and decreased expression of SIRT1. Exposure to VAT adipocytes caused more EC senescence-associated β-galactosidase activity than SAT adipocytes, an effect reduced in the presence of vascular endothelial growth factor A (VEGFA) neutralizing antibodies.

CONCLUSIONS—VAT-EC exhibit a more marked angiogenic and proinflammatory state than SAT-EC. This phenotype may be related to premature EC senescence. VAT-EC may contribute to hypoxia and inflammation in VAT. ***Diabetes*** **59:2755–2763, 2010**

From the [1]Institut National de la Santé et de la Recherche Médicale (INSERM), U858, Institut de Médecine Moléculaire de Rangueil, Toulouse, France, and Université Paul Sabatier Toulouse-III, Toulouse, France; the [2]Laboratoires Sérobiologiques, Division of Cognis, Pulnoy, France; the [3]Chirurgie Générale et Digestive, CHU Purpan, Toulouse, France; and the [4]Robert and Arlene Kogod Center on Aging, Mayo Clinic, Rochester, Minnesota.

Corresponding author: Anne Bouloumié, anne.bouloumie@inserm.fr.

Received 23 March 2010 and accepted 28 July 2010. Published ahead of print at http://diabetes.diabetesjournals.org on 16 August 2010. DOI: 10.2337/db10-0398.

The endothelium plays a major role in regulating the exchange of leukocytes, nutrients, and oxygen between blood and tissues. The extent of the capillary network and endothelial cell (EC) characteristics are major determinants of growth and function of adipose tissue (AT) (1). Indeed, angiogenesis and adipogenesis have been shown, through distinct approaches, to be tightly linked (2–4). Moreover, lipogenesis is dependent on lipoprotein lipase (LPL) and the newly discovered endothelial cell-surface glycoproteins, glycosylphosphatidylinositol-anchored HDL binding protein 1 (GPIHBP1), which are anchored to the EC that line the luminal surface of capillaries (5,6). Additionally, a recent study demonstrated that endothelial targeting of peroxisome proliferator-activated receptor gamma (PPARγ) regulates the metabolic response to high-fat diet in mice (7). Little is known about regional variations in the properties of fat tissue EC. Given their central role in lipid metabolism and inflammation, we tested the hypothesis that EC and their microenvironments differ among human fat depots in obesity.

We tested our hypothesis by comparing abdominal subcutaneous to omental EC isolated in parallel from the same obese human subjects for the following reasons: *1*) These two depots are highly clinically relevant, with omental fat more heavily implicated in metabolic syndrome and adverse clinical consequences of obesity than subcutaneous fat (8). *2*) Omental fat becomes more extensively infiltrated with immuno-inflammatory cells, including macrophages and T-lymphocytes, than subcutaneous fat in obesity (9–12). *3*) More is known about the differences in metabolism, fatty acid handling, gene expression, and mechanisms of growth in these two depots in humans with obesity than most other depots (13,14). *4*) These two depots differ in fat cell size in response to obesity as well as to lipogenesis and lipolysis (15,16).

We found that EC isolated from omental fat had reduced expression of genes related to metabolism and increased expression of genes related to angiogenesis and inflammation compared with subcutaneous cells. Conditioned medium prepared from fat cells of these two depots from obese subjects have distinct effects on EC from lean subjects. We found that cellular senescence, a proinflammatory state, is more evident in omental than subcutaneous fat-derived EC, possibly contributing to regional variations in fat tissue function.

RESEARCH DESIGN AND METHODS

Materials. Collagenase type 1 was purchased from Worthington Biochemical (Lakewood, NJ). Kits for $CD34^+$ and $CD31^+$ cells were, respectively, from StemCell Technologies (Grenoble, France) and Dynal-Biotech (Invitrogen, Cergy-Pontoise, France). Culture media, including endothelial cell basal medium (ECBM), were from Promocell (Heidelberg, Germany). Antibodies for flow cytometry were from BD Biosciences (Le Pont-de-Claix, France) or Caltag (Invitrogen, Cergy-Pontoise, France). Antibodies for immunofluorescence were from Dakocytomation (Denmark, CD31), Epitomics (CD34), Zymed (Invitrogen, France, ICAM1), Santa-Cruz (Cliniscience, France, GPIHBP1), Upstate (Millipore, France, phospho-histone-γ-H2AX), and Molecular Probes (Invitrogen; secondary antibodies coupled to AlexaFluor-488 or AlexaFluor-546). Chemicals were from Sigma (Saint-Quentin-Fallavier, France).

Subjects and isolation of mature adipocytes, stromal-vascular fraction cells, and EC from human subcutaneous and visceral AT (SAT and VAT). Paired biopsies from abdominal SAT (periumbilical) or VAT (greater omental) were obtained from subjects undergoing bariatric surgery for obesity. Subjects had been weight stable for at least 3 months before surgery, and they included 29 women and 1 man (mean BMI ± SEM = 43.35 ± 1.05 kg/m^2, range 34.5–59.1; mean age ± SEM = 40.4 ± 1.93 years, range 26–61 years). All subjects gave informed consent. Five subjects were hypertensive, 6 had hypercholesterolemia, and 3 had type 2 diabetes. The mean time since obesity ± SEM had been diagnosed was 18.2 ± 1.4 years. Abdominal SAT were obtained from 51 nonobese healthy women undergoing plastic surgery for cosmetic purposes (mean BMI ± SEM = 23.11 ± 0.221, range 19.5–27.2; mean age ± SEM = 43.57 ± 1.753, range 24–74). Fat collection protocols were approved by the Institutional Research Board of Inserm and the Toulouse University Hospital Ethics Committee. AT (2–10 g) was processed immediately after removal. Adipocytes and stromal-vascular fraction (SVF) were obtained by collagenase digestion as previously described (10). After digestion and filtration of the adipocyte suspension (250-μm mesh nylon sieves), adipocytes were washed three times with Krebs-Ringer bicarbonate buffer supplemented with 10 mmol/l HEPES (KRBH) and 0.1% fatty acid-free BSA (pH = 7.4). Mature adipocytes were suspended in ECBM supplemented with 0.1% BSA (1/10, vol/vol). Five μL of cell suspension were transferred onto plastic slides. Three different calibrated fields were examined to measure adipocyte diameters using NIS software (Nikon, Champigny-sur-Marne, France). SVF cells were counted and analyzed by flow cytometry to determine the number of ECs. At least 100,000 cells (in 100-μl phosphate buffer saline [PBS]/0.5% BSA, 2 mmol/l EDTA) were incubated (for 20 min, at 4°C) with FITC-CD31 and PerCP-CD34 antibodies or the appropriate isotype controls. After washing, the labeled cells were analyzed by flow cytometry using a fluorescence-activated cell sorter calibur flow cytometer and Diva software (BD-Biosciences). When the quantity of SVF cells was sufficient (11 subjects, paired SAT and VAT), native $CD34^+/CD31^+$ cells (EC) were isolated by immunoselection/depletion as previously described (10). Mature adipocytes and EC were either lysed and stored at −20°C for mRNA extraction or further processed.

Mature adipocyte culture. SAT and VAT mature adipocytes were placed in fibrin gels (1.5 mg fibrinogen/ml ECBM supplemented with 25 units/ml thrombin; 1/3, vol/vol) and cultured in ECBM/0.1% BSA supplemented with 100 units/ml penicillin and 100 μg/ml streptomycin. After 24 h, the adipocyte-conditioned media were collected and frozen at −80°C.

SAT mature adipocytes were cultured in ECBM supplemented with 0.1% BSA, 100 units/ml penicillin, and 100 g/ml streptomycin in CLINIcell 25-culture cassettes (1/3, vol/vol) in normoxia or hypoxia chambers (1% O2; Sanyo, Avon, France). After 24 h, mature adipocytes were lysed and stored at −20°C for RNA extraction.

Immunohistochemistry analyses. Tissue immunofluorescent staining of human SAT and VAT cut into small pieces (0.5–1 mm^3) was performed. After fixation in paraformaldehyde 4% for 1 h and subsequent washing in PBS, AT pieces were incubated for 30 min in PBS/2% BSA in the presence of 0.1% Triton. For γ-H2AX staining, AT pieces were permeabilized for 5 min in 95% ethanol and 5% acetic acid, and then incubated for 30 min in Tris-buffered saline (TBS)/3% BSA. AT pieces were incubated for 1 h with primary antibody (CD31 [1/50], CD34 [1/200], ICAM1 [1/50], GPIHBP1 [1/40], γ-H2AX [1/200]). After several washings (PBS/0.2% Tween or TBS), AT pieces were incubated for 30 min in PBS/2% BSA/0.1% Triton or TBS/3% BSA and then incubated with the corresponding fluorescently-labeled secondary antibodies (AlexaFluor-488 or AlexaFluor-546, 1/200). After washing, AT pieces were incubated for 10 min with 10 μg/ml Hoescht 33342 to stain nuclei. They were placed between two mounting slides and examined with a fluorescence (Nikon) or confocal (Zeiss 510) microscope.

Quantification of phospho-γ-H2AX positive nuclei in human SAT and VAT was performed on three calibrated fields using NIS software (Nikon, Champigny-sur-Marne, France) and normalized to the total number of nuclei (Hoescht 33342 staining).

TABLE 1
Human SAT and VAT adipocyte sizes

	SAT (% ± SE)	VAT (% ± SE)	*P*
Adipocytes <60 μm	29.1 ± 3.6	33.8 ± 3.0	0.12 ns
Adipocytes >100 μm	33.2 ± 3.0	19.1 ± 2.2	0.0003**

Data are percentages ± SE of small (< 60 μm) and large adipocytes (100 μm) in paired samples of SAT and VAT from $n = 30$ subjects; $^*P < 0.05$; $^{**}P < 0.01$; paired *t* test between SAT and VAT; ns, not significant.

RNA isolation and real-time PCR. Total RNA was extracted from EC and mature adipocytes and real-time PCR analyses were performed as previously described (10). Primers (Taqman gene expression assays from Applied Biosystems, Lifetechnologies, France) are listed in the supplemental table in the online appendix available at http://diabetes.diabetesjournals.org.

Culture and treatment of SAT-EC. Senescence-associated-β-galactosidase (SA-β-gal) activity was determined in human SAT-EC isolated from nonobese healthy women (mean BMI ± SEM = 25.34 ± 1.033, range 22.0–28.5; mean age ± SEM = 48.5 ± 3.074, range 35–57) and treated or not with adipocyte-conditioned media from SAT and VAT (pretreated or not for 1 h with 1 μg/ml VEGFA neutralizing antibody [R&D systems, Lille, France], or with VEGFA [10 ng/ml; Peprotech, Levallois-Perret, France]). Cells were fixed (5 min, room temperature) in 0.5% glutaraldehyde, washed with PBS, and incubated at 37°C for 16 h with fresh SA-β-gal staining solution (1 mg/ml of 5-bromo-4-chloro-3-indolyl galactopyranoside in dimethylformamide) supplemented with 0.12 mmol/l potassium ferrocyanide, 0.12 mmol/l potassium ferricyanide, and 1 mmol/l $MgCl_2$ (pH 6). The enzymatic reaction was stopped with water. Cells

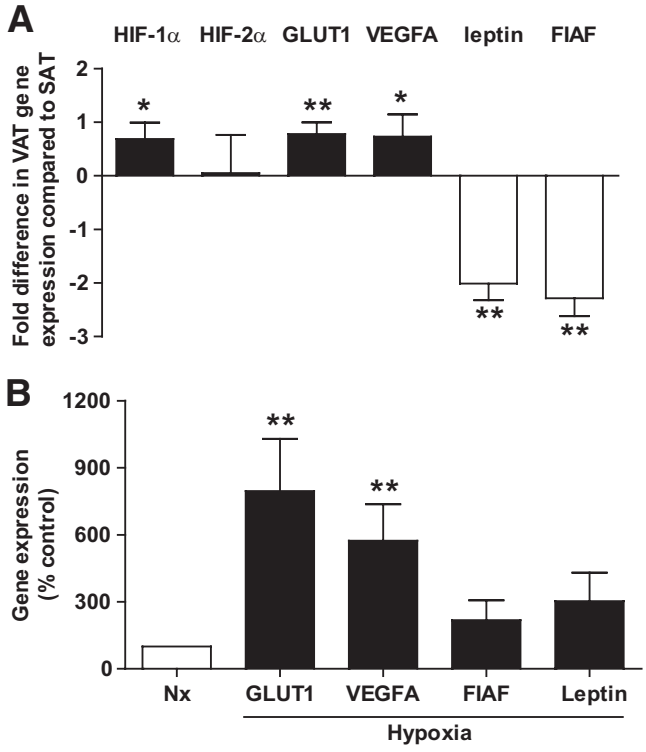

FIG. 1. Hypoxia-related genes in human SAT and VAT adipocytes. *A*: Comparison of mature adipocyte gene expression in SAT and VAT ($n = 30$). Hypoxia inducible factor 1 or 2, α subunit (HIF-1α, HIF-2α), GLUT1, vascular endothelial growth factor A (VEGFA), and fasting-induced adipose factor (FIAF). *Open bars*: genes upregulated, and *solid bars*: genes downregulated in VAT compared with SAT. Results are expressed as fold differences between VAT and SAT as means ± SEM. $^*P < 0.05$, $^{**}P < 0.01$; paired *t* tests between SAT and VAT. *B*: SAT adipocyte gene expression under normoxic (Nx) and hypoxic conditions (1% O_2) ($n = 6$). *Open bars*: gene expression under normoxic conditions, and *solid bars*: gene expression under hypoxic conditions. Results are expressed as means ± SEM $^{**}P < 0.01$; paired *t* tests between normoxic and hypoxic conditions.

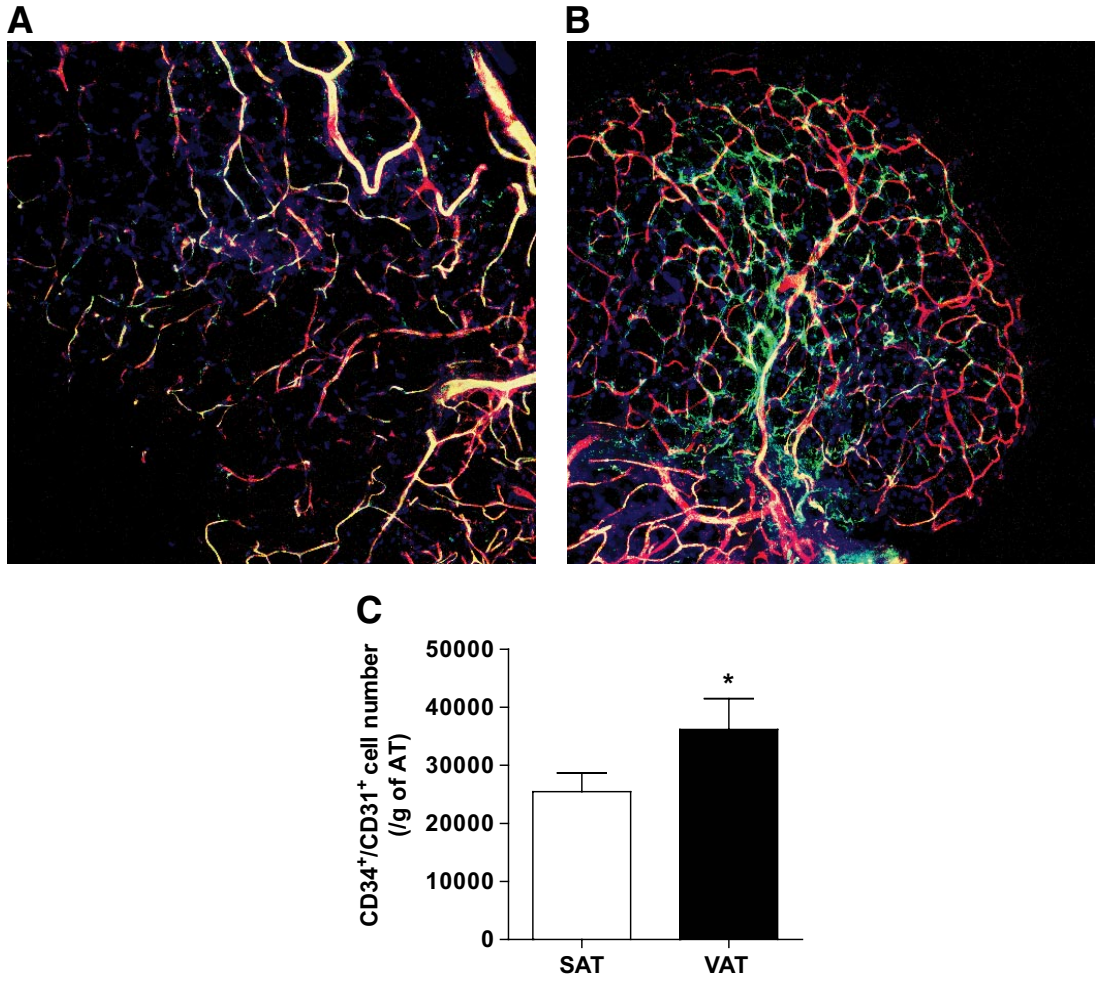

FIG. 2. Vascular network and EC number in human SAT and VAT. *A* and *B*: Representative photomicrographs of three-dimensional confocal immunofluorescence analyses of human (*A*) SAT and (*B*) VAT using antibodies directed against CD34 (green) and CD31 (red) ($n = 5$). Original magnification ×10. *C*: Flow cytometry analyses were performed on freshly harvested SVF using fluorescently-labeled antibodies directed against CD34 and CD31 ($n = 30$). *Open bar*: SAT, and *solid bar*: VAT. Results are means ± SEM of the number of $CD34^+/CD31^+$ cells per gram of AT *$P < 0.05$; paired *t* tests between the two AT depots. (A high-quality digital representation of this figure is available in the online issue.)

positive for SA-β-gal activity were counted by phase contrast microscopy through scanning the whole well and normalized to the total number of cells determined in four different fields with Hoescht 33342 nuclear staining using NIS software.

Statistical analyses. Statistical analyses were performed with GraphPad Software (San Diego, CA). Values are expressed as means ± SEM of (n) independent experiments. Correlations were determined with the Spearman test. Comparisons between the two groups (paired biopsies from SAT and VAT) were analyzed by paired Student *t* tests. Comparisons among groups were made by one-way ANOVA followed by a Dunnett post hoc test. Differences were considered significant when $P < 0.05$.

RESULTS

Adipocyte size and hypoxia-related gene expression in human subcutaneous and visceral AT (SAT and VAT). Human mature adipocytes were isolated from paired biopsies of SAT and VAT from obese subjects. Adipocytes were classified according to their diameter (i.e., small, with a diameter less than 60 μm; and large, with a diameter more than 100 μm) and the expression of genes was analyzed by real-time PCR. The proportion of large adipocytes was higher in SAT than VAT (Table 1). Expression of hypoxia-related genes, such as hypoxia-inducible factor (HIF)-1α, and certain HIF1-responsive genes (vascular endothelial growth factor A [VEGFA] and GLUT1, was higher in VAT than SAT adipocytes (Fig. 1*A*). In contrast, other genes regulated by hypoxic conditions and induced by HIF-1α, including leptin and the fasting-induced adipose factor (FIAF), exhibited the inverse profile (Fig. 1*A*). To further define the impact of hypoxia and adipocyte size on adipocyte gene expression, correlations among transcript levels and percentages of large adipocytes were calculated. Adipocyte transcript levels of VEGFA and GLUT1 were positively correlated with HIF1-α mRNA, irrespective of fat depot origin (*$P = 0.03$; Spearman $r = 0.2425$, $n = 60$ [SAT and VAT]; and **$P < 0.0001$; Spearman $r = 0.4744$, $n = 60$ [SAT and VAT], respectively). However, leptin and FIAF mRNAs were positively correlated with the percentage of large adipocytes (*$P = 0.012$; Spearman $r = 0.3302$, $n = 60$ [SAT and VAT]; and *$P = 0.014$; Spearman $r = 0.3231$, $n = 60$ [SAT and VAT], respectively). No correlation was found between the percentage of large adipocytes and transcript levels of HIF-1α, GLUT1, or VEGFA. Finally, the specific impact of low oxygen tension on adipocyte VEGFA and GLUT1 expression was confirmed by real-time PCR analysis of mature SAT adipocytes maintained in culture for 24 h under normoxic or hypoxic (1% O_2) conditions. VEGFA and GLUT1 transcript levels were increased under hypoxic culture conditions, whereas leptin and FIAF were not

altered substantially (Fig. 1*B*). Thus, human VAT adipocytes exhibit hypoxia-related characteristics, with increased HIF-1α, VEGFA, and GLUT1 expression, independently of fat cell size.

Vascular network and EC abundance in human SAT and VAT. To test whether a less extensive vascular network in VAT contributes to higher hypoxia-related gene expression in VAT than SAT in obese subjects, SAT and VAT were analyzed using three-dimensional confocal immunofluorescence microscopy for the EC markers CD34 and CD31. The apparent density of the vascular network, determined from colocalized CD34 and CD31 positive signals, was greater in VAT than SAT (Fig. 2*B* and *A*, respectively). This was confirmed by flow cytometry of SVF from both depots. The number of $CD34^+/CD31^+$ cells, normalized for tissue weight, was significantly higher in VAT than SAT (Fig. 2*C*). Thus, capillary density is higher in human VAT than SAT in obese subjects. To note, the EC number in SAT of lean ($n = 42$) subjects was similar to that of obese subjects (20,378 ± 2,554 vs. 25,476 ± 3,211 cells/g AT, respectively; $P = 0.1$), indicating that growth of SAT is associated with concomitant expansion of its capillary network.

The EC phenotype of human SAT and VAT. To determine whether hypoxia-related gene expression in VAT adipocytes is related to endothelial dysfunction, native human $CD34^+/CD31^+$ cells were isolated by immunoselection/depletion from SAT and VAT from obese subjects in biopsies that were of sufficient size. Genes involved in inflammation (chemokines and adhesion molecules), angiogenesis, metabolism, and cellular senescence were analyzed by real-time PCR. Many of the genes encoding proinflammatory and angiogenic factor receptors were upregulated in VAT compared with SAT-EC, including CC motif ligand 20 (CCL20), chemokine CXC motif ligand 8 (CXCL8), intercellular adhesion molecule-1 (ICAM1), vascular endothelial growth factor receptor 2 (VEGFR2), leptin receptor (Leptin R), and neuropilin 1 and neuropilin 2 (NRP1 and NRP2; Fig. 3*A* and *B*, respectively). Expression of genes involved in metabolism, such as endothelial lipase (EL), LPL, PPARγ, and GPIHBP1, tended to be higher in SAT than VAT-EC, although differences for EL and LPL did not reach statistical significance (Fig. 3*C*). Immunohistochemical analyses confirmed the increased expression of ICAM1 and decreased expression of GPIHBP1 in EC from VAT compared with SAT in obese subjects (Fig. 4*B* and *C*, and Fig. 4*E* and *F*, respectively). To note, both proteins were expressed at similar levels in SAT from lean and obese subjects (Fig. 4*A* and *D*). Moreover, real-time PCR analyses performed on isolated SAT-EC from lean subjects ($n = 6$) did not differ substantially in CCL20, CXCL8, ICAM1, Leptin R, NRP2, and EL compared with obese SAT-EC (data not shown). Finally, expression of the deacetylase, SIRT1, was decreased, whereas insulin-like growth factor binding protein 3 (IGFBP3), a gene upregulated in senescent EC, was increased in VAT-EC from obese subjects compared with SAT-EC (Fig. 5*A* and *B*, respectively). No differences in SIRT1 and IGFBP3 expression were detected in SAT-EC from lean and obese subjects (data not shown). To test whether cellular senescence is more extensive in VAT than SAT-EC, immunofluorescence analyses were performed using an antibody directed against γ-H2AX, a marker of senescent nuclei. We observed γ-H2AX positive nuclei in both SAT and VAT (Fig. 5*C* and *D*, respectively), but at a higher density in VAT-EC (3.3-fold increase in VAT vs. SAT, $P = 0.0004$, $^{**}n = 10$).

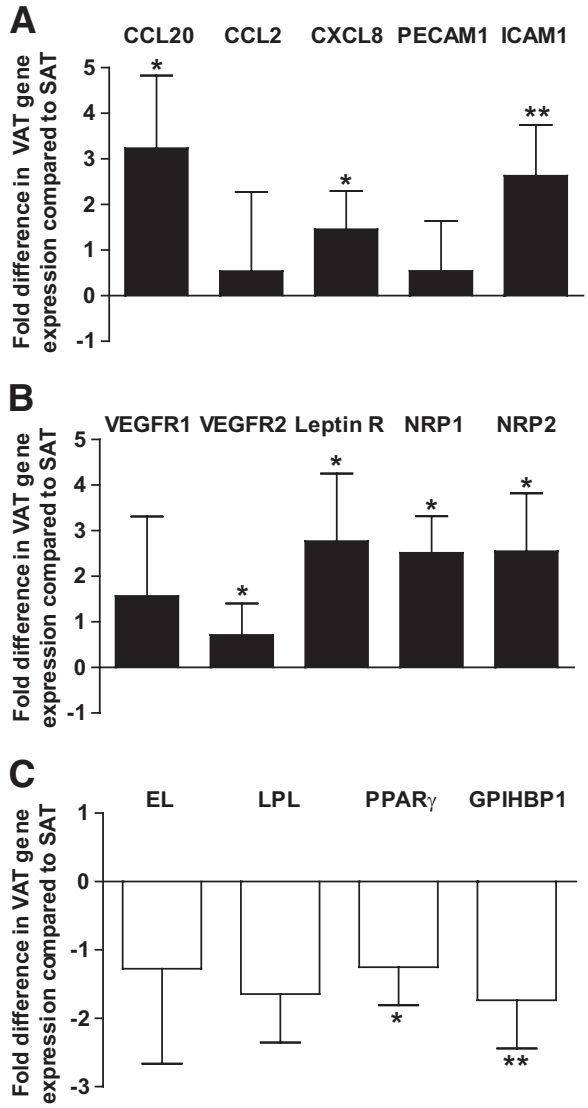

FIG. 3. Expression of inflammatory, angiogenic, and metabolic genes in human SAT and VAT EC. *A–C*: Comparison of SAT EC and VAT EC gene expression. CC motif ligand 20 (CCL20), CC motif ligand 2 (CCL2), chemokine CXC motif ligand 8 (CXCL8), platelet endothelial cell adhesion molecule-1 (PECAM1), intercellular adhesion molecule-1 (ICAM1), vascular endothelial growth factor receptor 1 and vascular endothelial growth factor receptor 2 (VEGFR1 and VEGFR2), leptin receptor (Leptin R), neuropilin 1 and neuropilin 2 (NRP1 and NRP2), endothelial lipase (EL), lipoprotein lipase (LPL), peroxisome proliferator-activated receptor gamma (PPARγ), and GPI-anchored HDL-binding protein 1 (GPIHBP1). *Open bars*: genes upregulated, and *solid bars*: genes downregulated in VAT compared with SAT. Results are expressed as fold differences between VAT EC and SAT EC as means ± SEM ($n = 7$ to 11) $^*P < 0.05$, $^{**}P < 0.01$; paired *t* tests between SAT EC and VAT EC.

Effects of the SAT and VAT microenvironment on senescence of human EC. To define effects of the SAT and VAT microenvironments on EC, native SAT-EC from nonobese women were treated with SAT and VAT adipocyte-conditioned media. Adipocyte-conditioned media clearly increased the number of SA-β-gal positive EC compared with control basal medium (Fig. 6*B* and *A*, respectively). Moreover, native SAT-EC treated with VAT conditioned medium developed a significantly higher percentage of senescent cells than the same native SAT-EC cells treated with SAT-derived conditioned medium (Fig.

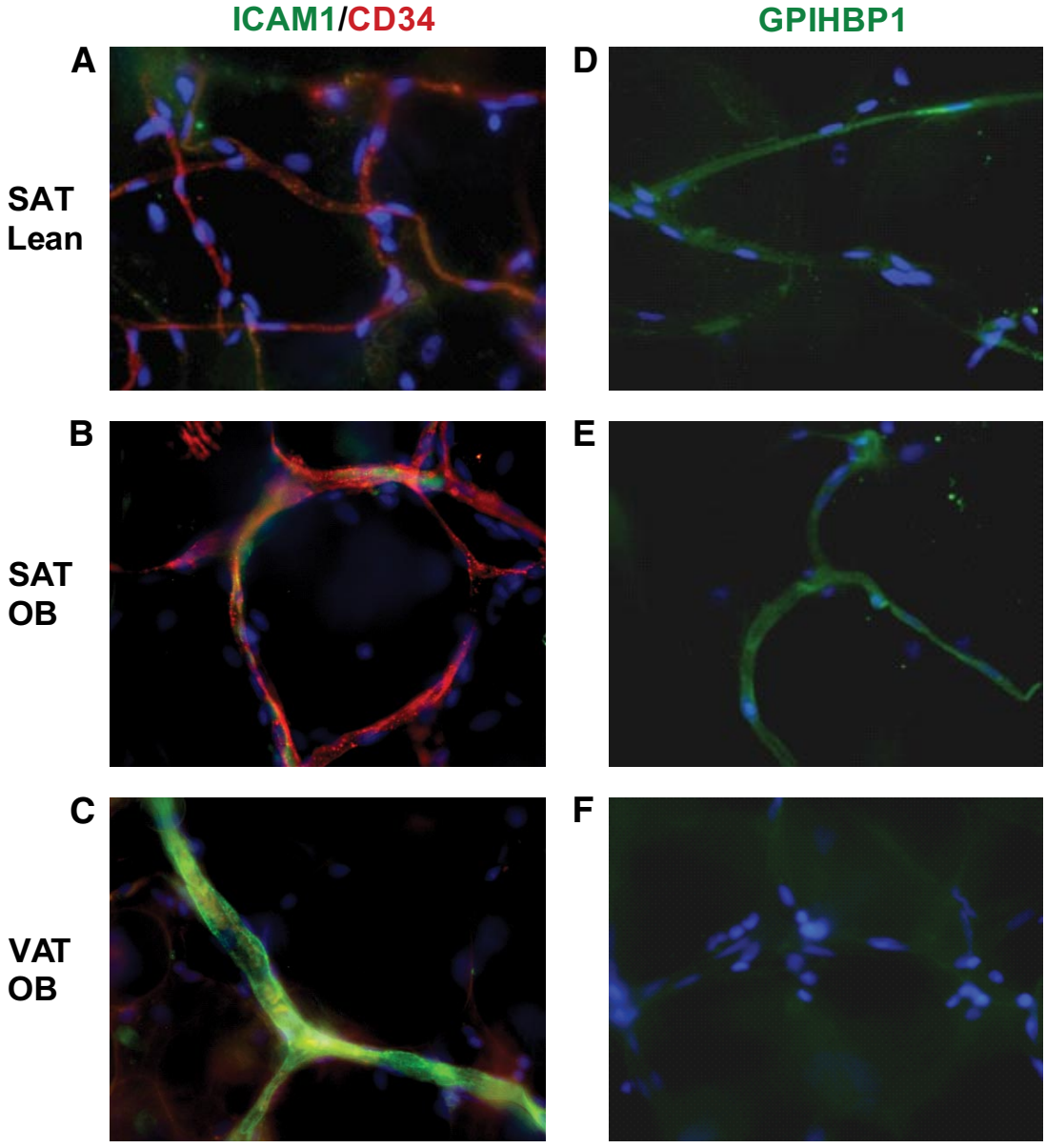

FIG. 4. Expression of ICAM1 and GPIHBP1 proteins in SAT and VAT. Representative photomicrographs of immunofluorescence analyses of human SAT from lean subjects (n = 4, 5) (*A* and *D*), obese subjects (n = 6, 9) (*B* and *E*) and VAT from obese subjects (n = 6, 9) (*C*, *F*) using antibodies directed against ICAM1 (green) and CD34 (red) (*A–C*) GPIHBP1 (green) (*D–F*) with nuclear staining with Hoescht 33342 (blue). Original magnification ×40. (A high-quality digital representation of this figure is available in the online issue.)

6*C*). EC proliferation was significantly increased by both SAT and VAT adipocyte-conditioned media, but to a greater extent in VAT than SAT-EC (Fig. 6*D*). Finally, to analyze the potential factor(s) involved in such a senescence-promoting effect of adipocyte-conditioned media, SAT-EC were treated with VEGFA alone or with SAT- and VAT-derived conditioned media in the presence of neutralizing VEGFA antibody. Although VEGFA increased the number of SA-β-gal positive EC, the presence of a neutralizing VEGFA antibody significantly reduced the effects of SAT- and VAT-conditioned media (Fig. 6*C*).

DISCUSSION

We found greater expression of hypoxia-related genes and smaller sizes of VAT than SAT adipocytes in obese subjects. The increased hypoxia in VAT is not likely to be a consequence of capillary rarefaction since vascular density, as well as EC number, were higher in VAT than SAT. However, the VAT-EC phenotype in obese subjects was markedly proangiogenic and inflammatory, with decreased expression of metabolism-related genes, including EL, GPIHBP1, and PPARγ. This phenotype of VAT-EC in obese subjects could be related to premature EC senescence, as suggested by expression of the senescence markers, IGFBP3 and γ-H2AX, as well as decreased expression of SIRT1.

AT is regionally distinct in terms of function, adipokine production, and inflammation. Adipocytes from VAT appear to have reduced capacity for lipogenesis (17) and greater capacity for lipolysis than SAT cells (15), with VAT containing more proinflammatory immune cells than SAT (12). In the present study and consistent with other reports (18,19), marked hypertrophy of SAT compared with VAT adipocytes was observed in obese subjects. Increased

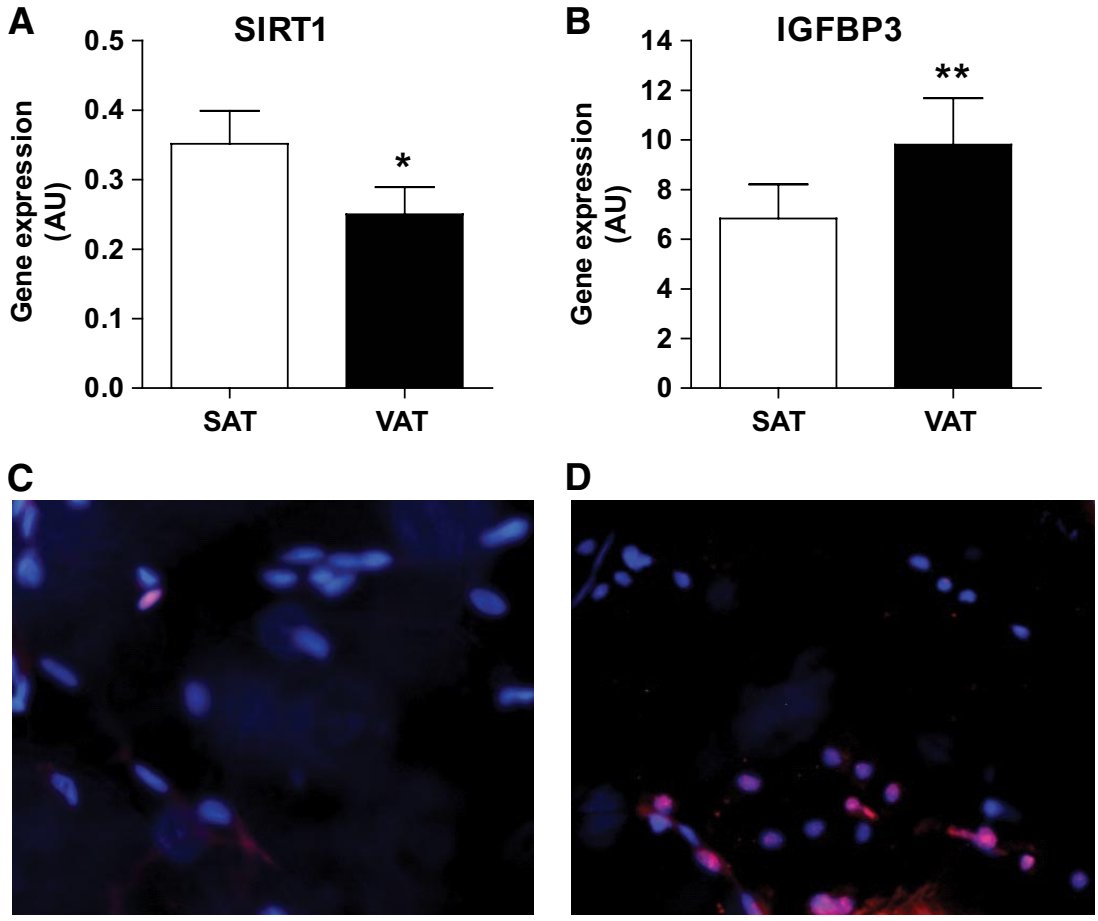

FIG. 5. Markers of senescence in native EC in SAT and VAT. *A–B*: Expression of (*A*) sirtuin 1 (SIRT1, $n = 9$) and (*B*) insulin-like growth factor binding protein 3 (IGFBP3, $n = 11$) in SAT EC and VAT EC. *Open bars*: SAT EC, and *solid bars*: VAT EC. Results are expressed as means ± SEM; *$P < 0.05$, **$P < 0.01$; paired *t* tests between SAT EC and VAT EC. *C–D*: Representative photomicrographs of immunohistofluorescence analyses of human (*C*) SAT and (*D*) VAT using antibody directed against phospho-γ-H2AX (red) and nuclear staining (blue) with Hoescht 33342 ($n = 10$). Original magnification ×40. (A high-quality digital representation of this figure is available in the online issue.)

expression of the hypoxia-related genes, HIF-1α, VEGFA, and GLUT1 was found in VAT compared with SAT adipocytes. Despite previous studies reporting that leptin and FIAF are induced under hypoxic conditions (20,21), we found they were lower in VAT than SAT. Irrespective of AT location, both leptin and FIAF transcript levels correlated with adipocyte size, as noted by others for leptin (22). Expression of VEGFA and GLUT1 was tightly linked with that of HIF-1α. Moreover, SAT adipocytes maintained under low oxygen conditions had higher VEGFA and GLUT1 expresssion than VAT, whereas the expression of both leptin and FIAF was not affected substantially. Together, the present results indicate that hypoxia-related processes are more highly activated in VAT than SAT and are not related to the extent of adipocyte hypertrophy in obese subjects. Moreover, qualitative analyses by confocal microscopy and flow cytometry, using both the EC markers CD34 and CD31 simultaneously, reveal that capillary network density was higher in VAT than in SAT. Therefore, hypoxia in VAT is unlikely to be a consequence of capillary rarefaction.

Treatment of native SAT-EC originating from normal nonobese women with conditioned media originating from VAT adipocytes from obese subjects led to marked proliferation compared with conditioned media from SAT adipocytes from the same subjects. This suggests that the microenvironment of VAT is more proangiogenic than SAT and is consistent with the greater capillary density in VAT than SAT. Whether increased proangiogenic induction by VAT adipocytes is related to hypoxia- and inflammation-related events remains to be determined. Our results indicate that VAT-EC from obese subjects exhibited a markedly proinflammatory and angiogenic activated state, with increased expression of chemokines, adhesion molecules, and angiogenic factor receptors. This phenotype could contribute to the greater abundance of proinflammatory immune cells in VAT than SAT (12). EL and GPIHBP1 are EC-specific metabolic genes, at least in murine models (23). Together with PPARγ (the main regulator of GPIHBP1), these genes were downregulated in VAT compared with SAT. A recent study in murine models of diet-induced obesity highlighted the key role of PPARγ in the modulation of EC function and metabolic alterations associated with obesity (7). Together our results show that although the capillary density of VAT is higher than that of SAT, VAT-EC exhibit a phenotype characterized by marked activation of inflammatory and angiogenic pathways associated with altered metabolic function in obese subjects.

This proangiogenic, proinflammatory phenotype might be related to premature endothelial cellular senescence. Indeed, senescent EC exhibit an activated state that may by induced either by extensive cell replication, leading to premature irreversible cell growth arrest, or by various

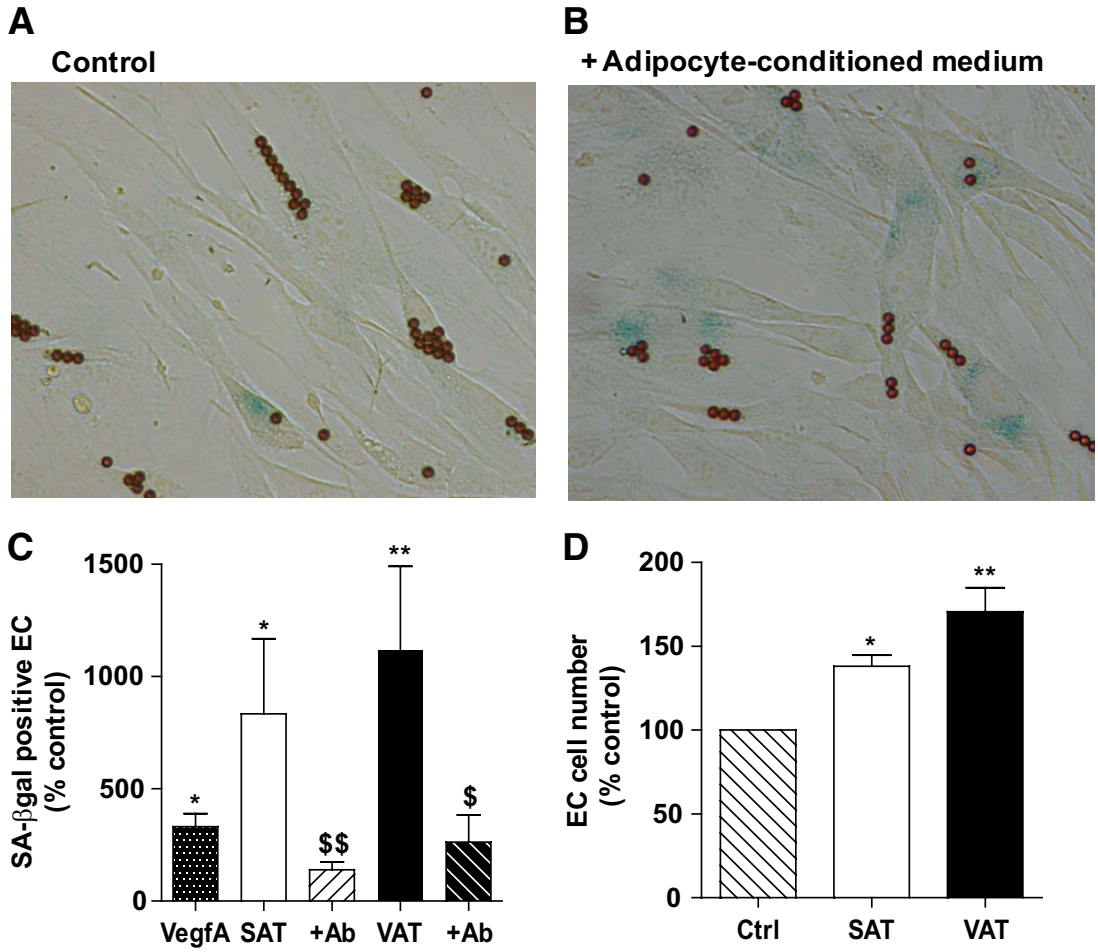

FIG. 6. Effect of the SAT and VAT microenvironment on EC senescence and proliferation. *A* and *B*: Representative photomicrographs of native SAT-EC cultured in the presence (*B*) or absence (*A*) of adipocyte-conditioned media ($n = 6$). Original magnification ×20. *C*: Percentage of SA-β-gal positive EC. Results are expressed as means ± SEM as percentages of control in the presence of VEGFA ($n = 3$) (*dotted*) or adipocyte-conditioned media from SAT (*open*) or VAT (*solid*) treated (*hatched*) or not with VEGFA neutralizing antibody ($n = 3$), *$P < 0.05$, **$P < 0.01$ vs. control; \$$P < 0.05$, \$\$$P < 0.01$, adipocyte-conditioned media alone versus containing VEGFA neutralizing Ab. *D*: Number of EC expressed as a percentage of control. *Hatched bar*: control, *open bar*: SAT, and *solid bar*: VAT. Results are expressed as means ± SEM as a percentage of control *$P < 0.05$, **$P < 0.01$, $n = 3$. (A high-quality digital representation of this figure is available in the online issue.)

stresses, including oxidative stress (24). Decreased expression of SIRT1, together with increased expression of IGFBP3 and γ-H2AX, have been noted in senescent, replicatively exhausted human EC (25–28), and we found indications of cellular senescence found in VAT-EC from obese subjects. Moreover, since conditioned media originating from VAT adipocytes increased the number of SA-β-gal positive EC, it is tempting to speculate that the chronic proangiogenic microenvironment of VAT promotes premature EC senescence, leading to endothelial dysfunction. Interestingly, VEGFA alone enhanced the number of SA-β-gal positive EC, although to a lesser extent than adipocyte-conditioned media. Moreover, neutralization of VEGFA reduced the senescence-promoting effect of the SAT and VAT adipocyte-conditioned media, suggesting that VEGFA might be an adipocyte-derived factor involved in premature adipose tissue EC senescence, consistent with its effects on EC senescence in other systems (29,30).

Cellular senescence in other cell types is associated with a senescent secretory phenotype, with increased production of proinflammatory cytokines, chemokines, and extracellular matrix-modifying proteins, as well as angiogenic factors (31–35). It will be important to define the secreted protein profile of senescent VAT-EC and SAT-EC and to determine whether such a phenotype is involved in the accumulation of immuno-inflammatory cells. Consistent with this possibility, we previously showed that treatment of SAT-EC with SAT adipocyte-conditioned media led to increased diapedesis of blood-derived monocytes (10).

The subjects in our study were obese. Whether regional variation in fat tissue EC properties are already present in lean subjects or arise as a consequence of obesity needs to be determined. Since cellular senescence is increased in obesity (36) and since obesity is associated with aortic endothelial cell senescence (37), it is tempting to speculate that obesity could induce senescence in VAT-EC to a greater extent than in SAT-EC. Consistent with this speculation, our study shows that SAT-EC from lean and obese subjects did not exhibit marked phenotypic differences or numbers relative to AT weight. If comparative studies of VAT-EC from lean and obese subjects validate our speculation, interventions that limit the accumulation of senescent EC or their proinflammatory state could improve the approaches to limit inflammation attributable to obesity and its complications.

ACKNOWLEDGMENTS

This study was supported by grants from INSERM (AVENIR), the Agence Nationale de la Recherche (ANR "RIOMA"), the European Union (FP7 ADAPT HEALTH-F2-2008-2010), the Laboratoires Sérobiologiques Division of COGNIS, NIH grants AG13925 and AG031736 (J.L.K.), the Noaber Foundation (J.L.K.), and the Ted Nash Long Life Foundation (to J.L.K.). This work was sponsored by the University Hospital of Toulouse (regulatory and ethics submission No. 06 029 03).

No potential conflicts of interest relevant to this article were reported.

A.V. researched data, wrote the manuscript, and contributed to discussion. J.G. researched data, reviewed/edited manuscript, and contributed to discussion. P.D., D.E., M.-A.M., C.S., and P.C. researched data. T.T., M.L., and J.L.K. reviewed/edited the manuscript and contributed to discussion. A.B. researched data, wrote the manuscript, reviewed/edited the manuscript, and contributed to discussion.

The authors thank Bénarous, MD, plastic surgeon, Clinique du Parc, Toulouse, France, for his technical support. The authors are also grateful for the excellent technical support and advice of B. Payre and Romina D'Angelo, Cellular Imaging Facility IFR150-Rangueil/TRI Plateform, Toulouse, France, for confocal microscopy.

REFERENCES

1. Rutkowski JM, Davis KE, Scherer PE. Mechanisms of obesity and related pathologies: the macro- and microcirculation of adipose tissue. FEBS J 2009;276:5738–5746
2. Rupnick MA, Panigrahy D, Zhang CY, Dallabrida SM, Lowell BB, Langer R, Folkman MJ. Adipose tissue mass can be regulated through the vasculature. Proc Natl Acad Sci U S A 2002;99:10730–10735
3. Brakenhielm E, Cao R, Gao B, Angelin B, Cannon B, Parini P, Cao Y. Angiogenesis inhibitor, TNP-470, prevents diet-induced and genetic obesity in mice. Circ Res 2004;94:1579–1588
4. Neels JG, Thinnes T, Loskutoff DJ. Angiogenesis in an in vivo model of adipose tissue development. FASEB J 2004;18:983–985
5. Beigneux AP, Davies BS, Gin P, Weinstein MM, Farber E, Qiao X, Peale F, Bunting S, Walzem RL, Wong JS, Blaner WS, Ding ZM, Melford K, Wongsiriroj N, Shu X, de Sauvage F, Ryan RO, Fong LG, Bensadoun A, Young SG. Glycosylphosphatidylinositol-anchored high-density lipoprotein-binding protein 1 plays a critical role in the lipolytic processing of chylomicrons. Cell Metab 2007;5:279–291
6. Beigneux AP, Davies BS, Bensadoun A, Fong LG, Young SG. GPIHBP1, a GPI-anchored protein required for the lipolytic processing of triglyceride-rich lipoproteins. J Lipid Res 2009;50 Suppl:S57–S62
7. Kanda T, Brown JD, Orasanu G, Vogel S, Gonzalez FJ, Sartoretto J, Michel T, Plutzky J. PPARγ in the endothelium regulates metabolic responses to high-fat diet in mice. J Clin Invest 2009;119:110–124
8. Jensen MD. Role of body fat distribution and the metabolic complications of obesity. J Clin Endocrinol Metab 2008;93:S57–S63
9. Cancello R, Tordjman J, Poitou C, Guilhem G, Bouillot JL, Hugol D, Coussieu C, Basdevant A, Bar Hen A, Bedossa P, Guerre-Millo M, Clement K. Increased infiltration of macrophages in omental adipose tissue is associated with marked hepatic lesions in morbid human obesity. Diabetes 2006;55:1554–1561
10. Curat CA, Miranville A, Sengenes C, Diehl M, Tonus C, Busse R, Bouloumie A. From blood monocytes to adipose tissue-resident macrophages: induction of diapedesis by human mature adipocytes. Diabetes 2004;53:1285–1292
11. Kintscher U, Hartge M, Hess K, Foryst-Ludwig A, Clemenz M, Wabitsch M, Fischer-Posovszky P, Barth TF, Dragun D, Skurk T, Hauner H, Bluher M, Unger T, Wolf AM, Knippschild U, Hombach V, Marx N. T-lymphocyte infiltration in visceral adipose tissue: a primary event in adipose tissue inflammation and the development of obesity-mediated insulin resistance. Arterioscler Thromb Vasc Biol 2008;28:1304–1310
12. Duffaut C, Zakaroff-Girard A, Bourlier V, Decaunes P, Maumus M, Chiotasso P, Sengenes C, Lafontan M, Galitzky J, Bouloumie A. Interplay between human adipocytes and T lymphocytes in obesity. CCL20 as an adipochemokine and T lymphocytes as lipogenic modulators. Arterioscler Thromb Vasc Biol 2009;29:1608–1614
13. Tchkonia T, Lenburg M, Thomou T, Giorgadze N, Frampton G, Pirtskhalava T, Cartwright A, Cartwright M, Flanagan J, Karagiannides I, Gerry N, Forse RA, Tchoukalova Y, Jensen MD, Pothoulakis C, Kirkland JL. Identification of depot-specific human fat cell progenitors through distinct expression profiles and developmental gene patterns. Am J Physiol Endocrinol Metab 2007;292:E298–E307
14. Caserta F, Tchkonia T, Civelek VN, Prentki M, Brown NF, McGarry JD, Forse RA, Corkey BE, Hamilton JA, Kirkland JL. Fat depot origin affects fatty acid handling in cultured rat and human preadipocytes. Am J Physiol Endocrinol Metab 2001;280:E238–E247
15. Arner P. Differences in lipolysis between human subcutaneous and omental adipose tissues. Ann Med 1995;27:435–438
16. Poulain-Godefroy O, Lecoeur C, Pattou F, Fruhbeck G, Froguel P. Inflammation is associated with a decrease of lipogenic factors in omental fat in women. Am J Physiol Regul Integr Comp Physiol 2008;295:R1–R7
17. Ortega FJ, Mayas D, Moreno-Navarrete JM, Catalan V, Gomez-Ambrosi J, Esteve E, Rodriguez-Hermosa JI, Ruiz B, Ricart W, Peral B, Fruhbeck G, Tinahones FJ, Fernandez-Real JM. The gene expression of the main lipogenic enzymes is downregulated in visceral adipose tissue of obese subjects. Obesity (Silver Spring) 18:13–20
18. Tchernof A, Belanger C, Morisset AS, Richard C, Mailloux J, Laberge P, Dupont P. Regional differences in adipose tissue metabolism in women: minor effect of obesity and body fat distribution. Diabetes 2006;55:1353–1360
19. Ledoux S, Coupaye M, Essig M, Msika S, Roy C, Queguiner I, Clerici C, Larger E. Traditional anthropometric parameters still predict metabolic disorders in women with severe obesity. Obesity (Silver Spring) 18:1026–1032
20. Ambrosini G, Nath AK, Sierra-Honigmann MR, Flores-Riveros J. Transcriptional activation of the human leptin gene in response to hypoxia. Involvement of hypoxia-inducible factor 1. J Biol Chem 2002;277:34601–34609
21. Wang B, Wood IS, Trayhurn P. Dysregulation of the expression and secretion of inflammation-related adipokines by hypoxia in human adipocytes. Pflugers Arch 2007;455:479–492
22. Jernas M, Palming J, Sjoholm K, Jennische E, Svensson PA, Gabrielsson BG, Levin M, Sjogren A, Rudemo M, Lystig TC, Carlsson B, Carlsson LM, Lonn M. Separation of human adipocytes by size: hypertrophic fat cells display distinct gene expression. FASEB J 2006;20:1540–1542
23. Davies BS, Waki H, Beigneux AP, Farber E, Weinstein MM, Wilpitz DC, Tai LJ, Evans RM, Fong LG, Tontonoz P, Young SG. The expression of GPIHBP1, an endothelial cell binding site for lipoprotein lipase and chylomicrons, is induced by peroxisome proliferator-activated receptor-γ. Mol Endocrinol 2008;22:2496–2504
24. Erusalimsky JD. Vascular endothelial senescence: from mechanisms to pathophysiology. J Appl Physiol 2009;106:326–332
25. Ota H, Akishita M, Eto M, Iijima K, Kaneki M, Ouchi Y. Sirt1 modulates premature senescence-like phenotype in human endothelial cells. J Mol Cell Cardiol 2007;43:571–579
26. Kim KS, Kim MS, Seu YB, Chung HY, Kim JH, Kim JR. Regulation of replicative senescence by insulin-like growth factor-binding protein 3 in human umbilical vein endothelial cells. Aging Cell 2007;6:535–545
27. d'Adda di Fagagna F, Reaper PM, Clay-Farrace L, Fiegler H, Carr P, Von Zglinicki T, Saretzki G, Carter NP, Jackson SP. A DNA damage checkpoint response in telomere-initiated senescence. Nature 2003;426:194–198
28. Geisel D, Heverhagen JT, Kalinowski M, Wagner HJ. DNA double-strand breaks after percutaneous transluminal angioplasty. Radiology 2008;248:852–859
29. Trivier E, Kurz DJ, Hong Y, Huang HL, Erusalimsky JD. Differential regulation of telomerase in endothelial cells by fibroblast growth factor-2 and vascular endothelial growth factor-a: association with replicative life span. Ann N Y Acad Sci 2004;1019:111–115
30. Kurz DJ, Hong Y, Trivier E, Huang HL, Decary S, Zang GH, Luscher TF, Erusalimsky JD. Fibroblast growth factor-2, but not vascular endothelial growth factor, upregulates telomerase activity in human endothelial cells. Arterioscler Thromb Vasc Biol 2003;23:748–754
31. Coppe JP, Patil CK, Rodier F, Sun Y, Munoz DP, Goldstein J, Nelson PS, Desprez PY, Campisi J. Senescence-associated secretory phenotypes reveal cell-nonautonomous functions of oncogenic RAS and the p53 tumor suppressor. PLoS Biol 2008;6:2853–2868
32. Krtolica A, Campisi J. Cancer and aging: a model for the cancer promoting effects of the aging stroma. Int J Biochem Cell Biol 2002;34:1401–1414
33. Parrinello S, Coppe JP, Krtolica A, Campisi J. Stromal-epithelial interactions in aging and cancer: senescent fibroblasts alter epithelial cell differentiation. J Cell Sci 2005;118:485–496

34. Passos JF, Nelson G, Wang C, Richter T, Simillion C, Proctor CJ, Miwa S, Olijslagers S, Hallinan J, Wipat A, Saretzki G, Rudolph KL, Kirkwood TB, von Zglinicki T. Feedback between p21 and reactive oxygen production is necessary for cell senescence. Mol Syst Biol 6:347
35. Xue W, Zender L, Miething C, Dickins RA, Hernando E, Krizhanovsky V, Cordon-Cardo C, Lowe SW. Senescence and tumour clearance is triggered by p53 restoration in murine liver carcinomas. Nature 2007; 445:656–660
36. Minamino T, Orimo M, Shimizu I, Kunieda T, Yokoyama M, Ito T, Nojima A, Nabetani A, Oike Y, Matsubara H, Ishikawa F, Komuro I. A crucial role for adipose tissue p53 in the regulation of insulin resistance. Nat Med 2009;15:1082–1087
37. Wang CY, Kim HH, Hiroi Y, Sawada N, Salomone S, Benjamin LE, Walsh K, Moskowitz MA, Liao JK. Obesity increases vascular senescence and susceptibility to ischemic injury through chronic activation of Akt and mTOR. Sci Signal 2009;2:ra11